Article

Insertion of an inorganic barrier layer as a method of improving the performance of quantum dot light-emitting diodes

Sang Hyun Yoon, Dham Gwak, Hong Hee Kim, Hwi Je Woo, Jinhee Cho, Jin Woo Choi, Won Kook Choi, Young Jae Song, Chang-Lyoul Lee, Jongnam Park, Kwang Heo, and Young Jin Choi

ACS Photonics, **Just Accepted Manuscript** • DOI: 10.1021/acsphotonics.8b01672 • Publication Date (Web): 12 Feb 2019

Insertion of an inorganic barrier layer as a method of improving the performance of quantum dot light-emitting diodes

Sang Hyun Yoon[1], Dham Gwak[1], Hong Hee Kim[2], Hwi Je Woo[3], Jinhee Cho[4], Jin Woo Choi[5], Won Kook Choi[2], Young Jae Song[6,7], Chang-Lyoul Lee[5], Jongnam Park[4], Kwang Heo[1], and Young Jin Choi[1,*]

[1]*Department of Nanotechnology & Advanced Materials Engineering, Sejong University, Seoul 05006, Republic of Korea*

[2]*Center for Opto-Electronic Materials and Devices, Korea Institute of Science and Technology, Seoul 02792, Republic of Korea*

[3]*SKKU Advanced Institute of Nanotechnology (SAINT), Sungkyunkwan University (SKKU), Suwon 16419, Republic of Korea*

[4]*Department of Energy & Chemical Engineering, Ulsan National Institute of Science and Technology, Ulsan 44919, Republic of Korea*

[5]*Advanced Photonics Research Institute (APRI), Gwangju Institute of Science and Technology (GIST), Gwangju 61005, Republic of Korea*

[6]*Department of Physics, Sungkyunkwan University (SKKU), Suwon 16419, Republic of Korea*

[7]*Department of Nano-engineering, Sungkyunkwan University (SKKU), Suwon 16419, Republic of Korea*

*Corresponding author. Email: jini38@sejong.ac.kr

Abstract

Quantum dot light-emitting diodes (QLEDs) are expected to be the basis of next-generation displays and have consequently been extensively investigated with the aim of commercialization. Herein, QLED brightness, efficiency, and lifetime are significantly improved by insertion of an Al_2O_3 barrier layer via atomic layer deposition (ALD), which effectively suppresses the etching reaction with poly(3,4-ethylenedioxytiophene):polystyrene sulfonate and prevents metal ion diffusion from ITO into the emission layer, thereby effectively reducing the effect of exciton quenching. The abovementioned suppression of exciton quenching is verified using time-resolved photoluminescence spectroscopy/energy-dispersive X-ray spectroscopy, and a device prepared using four ALD cycles is shown to exhibit increased maximal luminance (39,410 cd/m^2; two times the value achieved without the Al_2O_3 layer), current efficiency (47.89 cd/A; eight times the value achieved without the Al_2O_3 layer), and external quantum efficiency (12.89%). In addition, all Al_2O_3-

containing QLEDs feature longer lifetimes than the QLED without Al_2O_3.

Keywords: QLED, metal ion diffusion Al_2O_3, performance optimization, atomic layer deposition, barrier layer

Quantum dots (QDs) have been widely investigated as lighting materials because of their inherent advantages, e.g., size-dependent emission color, narrow emission bandwidth, good photostability, and compatibility with solution processing (1–4). Quantum dot light-emitting diodes (QLEDs), featuring a structure and carrier injection mechanism similar to those of organic light-emitting diodes (OLEDs), use QDs as an emissive layer (EML) instead of organic materials and exhibit high brightness and a wide color gamut (5–7). However, despite the excellent electro-optical characteristics of QLEDs, their commercialization is hindered by their low efficiency and lifetime. The efficiency degradation of QLEDs and OLEDs has been shown to originate from metal ion diffusion and migration (8), unbalanced rate of electron and hole injection (9–11), and Auger recombination (12). To improve the performance of QLEDs, many researchers have tried to balance the rates of electron and hole injection into the EML by inserting non-conductive materials as a carrier-blocking layer (10, 11, 13) and attempted to enhance charge transfer within the QD layer by shortening the length of QD-bound ligands to increase the QD packing density (14). In addition, various approaches such as core-shell alloy (12)/gradient shell (15) formation and change of shell thickness (3) have been adopted to reduce the amount of defects originating from the lattice mismatch at the core-shell interface in core-shell-structured QDs. In this study, we introduce a new approach to improving the performance of QLEDs and examine its practical applicability. In conventional QLEDs, which have a transparent anode/hole injection layer (HIL)/hole transport layer (HTL)/QD (EML)/electron transport layer (ETL)/high-reflectance low-work-function cathode structure, efficiency deterioration is mainly caused by exciton quenching due to anode-to-EML metal ion diffusion (8). For a typical combination of indium tin oxide (ITO) as an anode and poly(3,4-ethylenedioxytiophene):polystyrene sulfonate (PEDOT:PSS) as a HIL, metal ion diffusion into the polymer layer is initiated already during device fabrication, because sulfur contained in PEDOT:PSS etches the ITO anode (16). In addition, metal (i.e., In and Sn) ions easily migrate into the EML upon QLED operation under a high electric field. Herein, we try to solve this problem by inserting a barrier layer and thus preventing metal ion diffusion at the ITO-PEDOT:PSS interface.

Metal oxides have been widely investigated as barrier materials inhibiting the migration of In or Sn in ITO anodes of QD solar cells (17). Among metal oxides, Al_2O_3, which can be easily and quickly deposited through atomic layer deposition (ALD) at relatively low temperature using trimethylaluminum (TMA) and H_2O as precursors (18, 19) is known to be the most effective material for blocking metal ion migration. Moreover, the large band gap and deep valence band

level of Al_2O_3 allow it to be used as an encapsulation material (20), exciton quenching suppressor (21), and carrier blocking layer for hole/electron injection to balance the carrier injection rate in OLEDs (11) or QLEDs (13). The band gap of Al_2O_3 has been experimentally determined as 8.8 eV for α-Al_2O_3 (22), 7.1–8.7 eV for γ-Al_2O_3 (23, 24), and 5.1–7.1 eV for amorphous Al_2O_3 (24), depending on the synthesis method. In particular, ALD-deposited amorphous Al_2O_3 films typically exhibit band gaps of ~6.2 eV (25, 26). Conventional-structure QLEDs possess an excess of electrons, since the injection rate of electrons is higher than that of holes because of the difference of carrier mobility in the carrier transport layer. In a conventional QLED, the hole mobility of poly(9-vinylcarbazole) (PVK; 2.5×10^{-6} cm^2 V^{-1} s^{-1}), a typical HTL material, is three orders of magnitude lower than the electron mobility of ZnO (~1.8×10^{-3} cm^2 V^{-1} s^{-1}), a typical ETL material (10). So, the Al_2O_3 layer inserted at the ITO-PEDOT:PSS interface to hinder metal ion migration should (a) be as thin as possible in order not to prevent the injection of holes and allow their tunneling from ITO to PEDOT:PSS and (b) conformably cover the ITO surface to prevent the presumed reaction between ITO and PEDOT:PSS. In addition, ultrathin (≤1 nm) amorphous Al_2O_3 films typically feature narrow band gaps of 2.6–2.9 eV (27) and can therefore hardly act as a barrier to hole injection.

Herein, QLEDs with Al_2O_3 layers of various thickness were fabricated by varying the number of ALD cycles (*n*), and the greatest improvements in current efficiency and luminance were observed for n = 4. The peak values of luminance and current efficiency of the corresponding QLED were measured as 39,410 cd/m^2 and 47.89 cd/A, respectively, exceeding those of the Al_2O_3-free QLED by factors of two and eight, respectively. Furthermore, the insertion of an Al_2O_3 barrier layer also increased the lifetime of QLED devices.

Materials and methods

Before use, ITO-coated glass substrates were cleaned by sequential 15-min sonication in acetone, isopropyl alcohol, and deionized water. During ALD, TMA reacts with the surface OH groups through ligand exchange to produce O–Al bonds and release methane, and the high concentration of OH groups on the ITO surface allows for conformal coating. The cleaned ITO glass substrates were treated by UV-ozone for 20 min to increase the concentration of surface OH groups, and an Al_2O_3 barrier layer was then deposited by ALD (Lucida™ D100 ALD system, NCD) at 150 °C using TMA and H_2O as precursors. All subsequent layers except for the Al cathode were deposited by spin coating. PEDOT:PSS (Clevios AI 4083), PVK, and QDs (CdSe/ZnS core/shell) were purchased from Heraeus, Sigma-Aldrich, and ZEUS, respectively. A dispersion of ZnO nanoparticles (NPs, ~13 nm in size) in butanol was synthesized as described elsewhere (28). The concentrations of PVK (in chlorobenzene), QDs (in hexane), and ZnO NPs (in butanol) equaled 100, 10 and 20 mg/mL, respectively. Each layer was baked on a hot plate (130 °C, 30 min) to vaporize solvent and

create homogeneous films after spin-coating. Finally, the Al electrode (width = 3 mm, length = 12 mm) was deposited on ZnO in a thermal evaporator and patterned using a metal mask. The thicknesses of PEDOT:PSS, PVK, QDs, ZnO, and Al layers were measured as 20, 20, 20, 25, and 150 nm, respectively. QLED characteristics were monitored by a system comprising a luminance meter (Photo Research, Spectra Scan PR-670) and a source meter (KEITHLEY, 2400). The surface of Al_2O_3-coated ITO was investigated by scanning Kelvin probe microscopy (SKPM; Park systems NX10). The work functions of bare and Al_2O_3-coated ITO were calculated from the relative values of SKPM data by comparison with the values of highly oriented pyrolytic graphite, which has a work function of ~4.6 eV. The dynamics of QLED photoluminescence (PL) decay was investigated by time-resolved photoluminescence (TR-PL) measurements using a pulsed diode-laser head (LDH-P-C-405, PicoQuant) as the excitation source (excitation wavelength = 400 nm, repetition frequency = 10 MHz). PL emission was spectrally resolved using collection optics and a monochromator (SP-2150i, Acton), and the corresponding time-resolved signal was recorded by a TR-PL module (PicoHarp 300, PicoQuant) equipped with a micro-channel plate photomultiplier tube (MCP-PMT, R3809U-50, Hamamatsu). The total instrument response function (IRF) was less than 140 ps, and temporal resolution equaled 16 ps. Deconvolution of the PL decay curve for separating the IRF from the actual PL decay signal was performed using FluoFit software (PicoQuant) to infer the time constant associated with each exponential decay curve.

Results and discussion

Figure 1 shows a schematic energy diagram of our green-emitting QLED with conventional structure, highlighting the presence of an Al_2O_3 layer at the ITO-PEDOT:PSS interface as a barrier to metal ion diffusion. To efficiently prevent metal ion diffusion at the above interface, the Al_2O_3 layer must satisfy two conditions. First, since Al_2O_3 has poor carrier injection properties in terms of QLED band alignment, this layer should be as thin as possible to allow for easy charge carrier injection through tunneling. Second, Al_2O_3 should fully cover the ITO electrode to prevent its surface from being etched by PEDOT:PSS during device fabrication. In view of the above, we tried to optimize the thickness of the Al_2O_3 layer by varying *n* to satisfy both conditions.

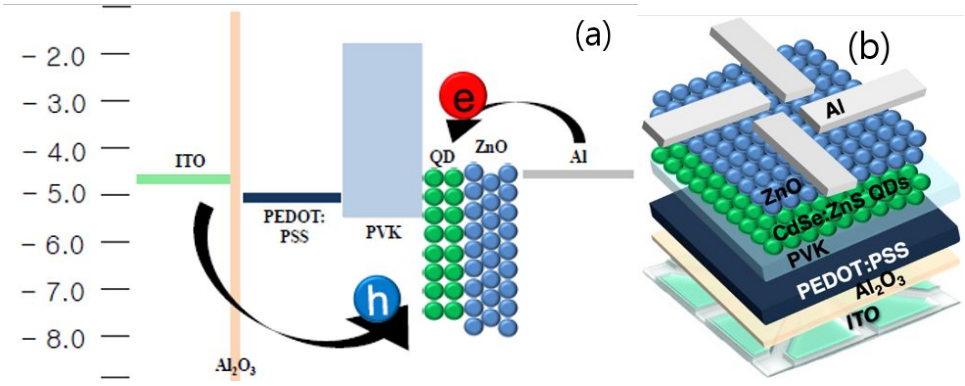

Figure 1. Schematic diagram of QLED (a) energy band alignment and (b) structure.

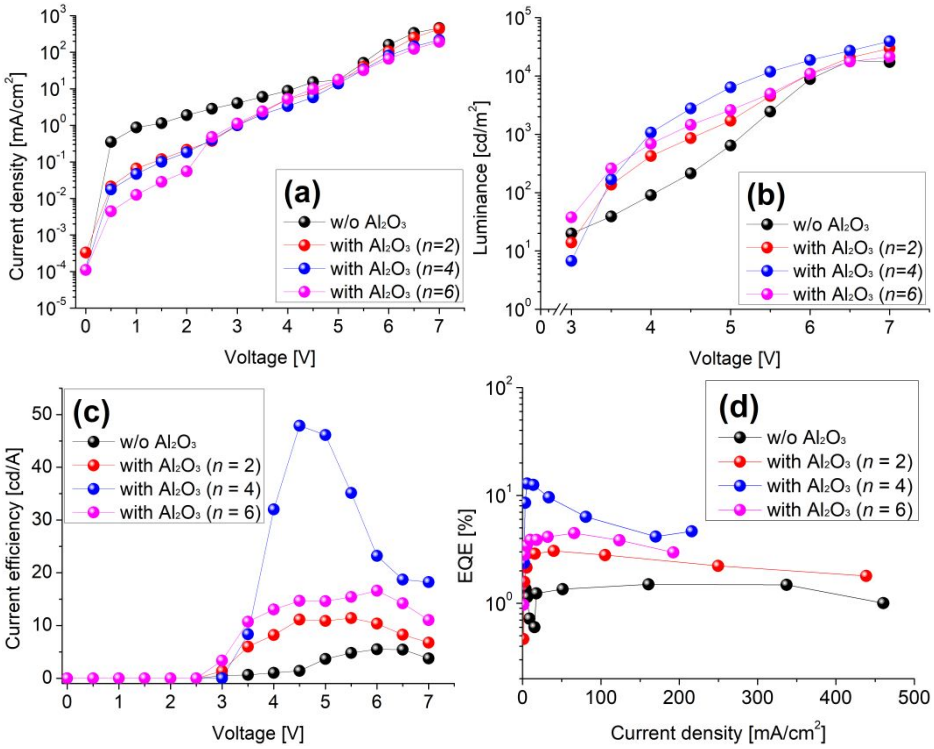

Figure 2. EL properties of QLEDs fabricated using n = 2, 4, and 6. (a) Voltage vs. current density, (b) voltage vs. luminance, (c) voltage vs. current efficiency, and (d) current density vs. external quantum efficiency (EQE) plots.

Figure 2(a) shows the current density vs. bias voltage (*J*-*V*) plots of QLEDs with different n, revealing that current density decreased with increasing n. This behavior was explained by the fact that the number of carriers injected into the EML decreased with increasing thickness of Al_2O_3, which acted as a charge carrier injection barrier. In the ALD process, the growth per cycle (GPC) is not constant but varies in each cycle depending on the growth conditions (i.e., occurrence of self-terminating reactions, growth temperature, and concentration of surface hydroxyl groups) (19). Assuming the commonly accepted GPC for Al_2O_3 of 1–1.5 Å/cycle (11, 13, 29), the deposited Al_2O_3 layer was calculated to be thinner than 1 nm, although the nm-scale surface roughness of ITO did not allow the barrier layer thickness to be measured experimentally. However, the decrease of current density with increasing n was attributed to the concomitant increase in the thickness of the insulating Al_2O_3. **Figure 2(b)** shows the luminance vs. voltage (*L*-*V*) plots for QLEDs with different n, demonstrating that the highest luminance (39,410 cd/m^2 at an applied voltage of 7 V) was observed for four cycles and exceeded that of an Al_2O_3-free device (18,300 cd/m^2) by a factor of more than two. Devices fabricated using n = 2 and 6 also showed improved luminance characteristics compared with the QLED without Al_2O_3. In particular, the luminance of the Al_2O_3-free QLED at a bias of 7 V was less than that at a bias of 6.5 V, which was ascribed to external quantum efficiency (EQE) roll-off at high current density (**Figure S1**). On the contrary, as the bias was raised from 6.5 to 7 V, the luminance of QLEDs with Al_2O_3 continuously increased even in the

case of the n = 2 device, which featured a current density similar to that of the Al_2O_3-free QLED in the bias range of 6.5–7 V. These results suggested that the incorporation of the Al_2O_3 layer can solve the problem of EQE reduction at high current densities.

Figure 2(c) shows the current efficiency of QLED devices as a function of applied voltage and n, revealing that the best performance was observed at n = 4. Current efficiency is closely related to the balance between electron and hole injection (4, 10). In view of the fact that convectional QLEDs with an Al/ZnO/QDs/PVK/PEDOT:PSS/ITO structure are characterized by the natural presence of excessive electrons, layers of insulators such as Al_2O_3 have generally been inserted between the cathode and EML to improve device efficiency by balancing charge carrier injection. Thus, the incorporation of an additional layer of Al_2O_3 between the anode and EML should block hole transfer from the electrode to the QD layer and hence decrease current efficiency. As expected, the QLED fabricated using n > 50 (Al_2O_3 layer thickness > 5 nm) did not emit any light. However, the charge blocking characteristics of the Al_2O_3 film were strikingly different in the ultra-thin regime, as highlighted by the fact that the current efficiency of QLEDs with an ultra-thin Al_2O_3 layer increased with increasing n (up to n = 4), i.e., the ultra-thin Al_2O_3 layer did not act as a hole-blocking layer.

Figure 2(d) shows the EQE of our QLEDs as a function of current density and n, revealing that the highest value of 12.89%, observed for n = 4, was about eight times higher than that of the Al_2O_3-free QLED. This result shows that high EQE can be maintained at high current densities (>200 mA/cm^2). In particular, although the four-cycle QLED featured a relatively high rate of EQE reduction with increasing current density compared to other devices, it still showed higher EQE.

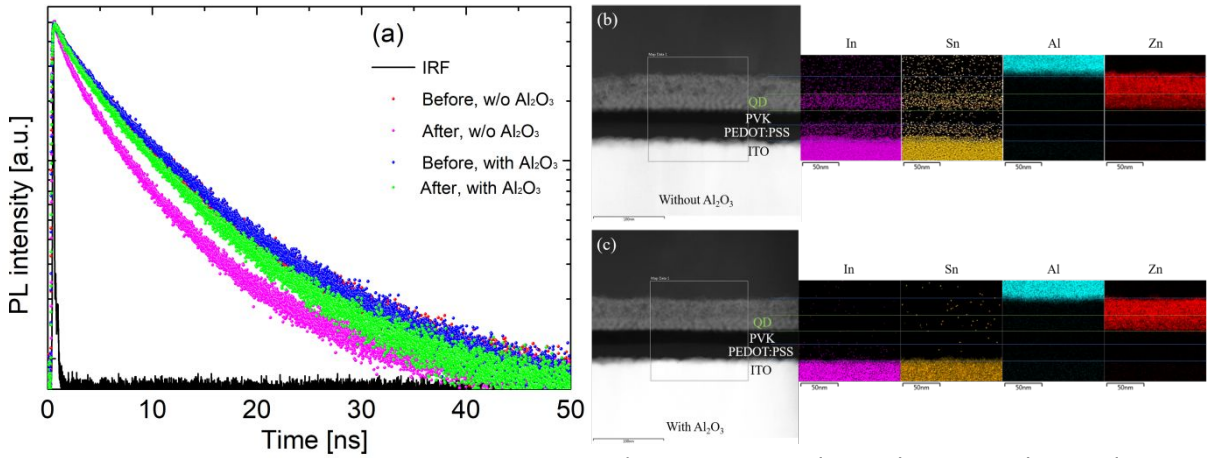

Figure 3. (a) PL decay dynamics observed before and after operation of QLEDs with or without an Al_2O_3 (n = 4) barrier layer. The black line represents the IRF. EDS mappings obtained after device operation for QLEDs without (b) and with (c) an Al_2O_3 barrier layer.

To verify the role of Al_2O_3 as a metal diffusion barrier during device operation, we used TR-PL

spectroscopy to examine exciton quenching phenomena, which can be enforced by metal ion diffusion. **Figure 3(a)** shows the PL decay dynamics observed before and after the operation of QLEDs with or without an Al_2O_3 (n = 4) barrier layer, and Table S1 summarizes the corresponding PL lifetimes and fractional intensities. Before operation, both devices showed similar PL lifetimes of ~8.4 ns, while a noticeable PL lifetime difference was detected after 5-min operation at maximum luminance. Under these conditions, the PL lifetime slightly dropped to 7.5 ns in the QLED with an Al_2O_3 (n = 4) layer, the Al_2O_3-free QLED exhibited a significantly shorter PL lifetime of 6.4 ns.

Subsequently, we examined the cross-sections of operated QLEDs by Energy-dispersive X-ray spectroscopy (EDS). As shown in **Figure 3(b)**, pronounced signals of In and Sn were observed in the QD EML as well as in the ITO electrode when no Al_2O_3 coating was applied. On the contrary, only weak In and Sn signals randomly spread over the whole device were observed for the Al_2O_3-coated QLED **(Figure 3(c))**. These weak signals might reflect the presence of impurities scattered by the ion beam during transmission electron microscopy (TEM) sample preparation. These results showed that the Al_2O_3 barrier can effectively suppress the effect of exciton quenching during device operation by blocking the migration of metal ions.

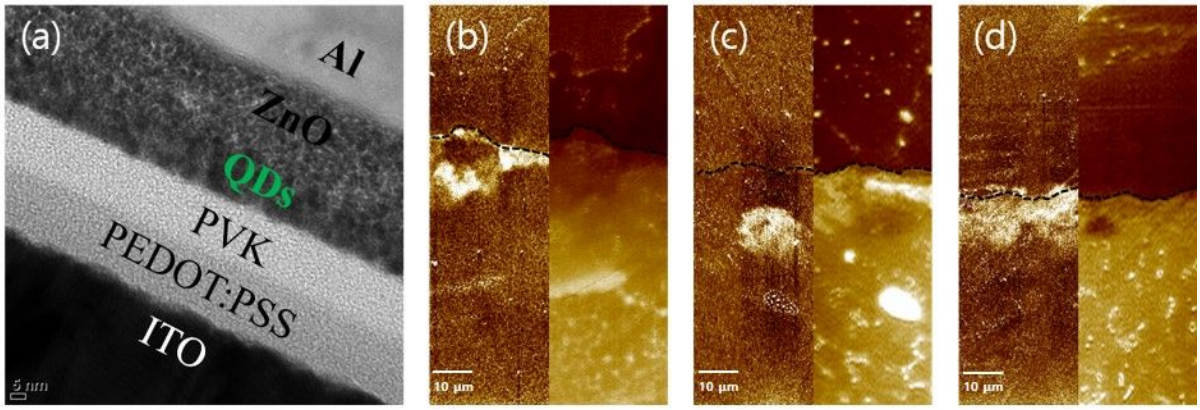

Figure 4. (a) Cross-sectional TEM image of a QLED with an Al_2O_3 barrier layer, (b–d) Surface morphology (left) and corresponding SKPM (right) images obtained at the boundary (marked by black dashed lines) between ITO and Al_2O_3-coated ITO for (b) n = 2, (c) n = 4, and (d) n = 6, respectively.

Figure 4(a) is a cross-sectional transmission electron microscopy (TEM) image of our QLED. We could resolve each layer except for the Al_2O_3 layer, which was impossible to identify because of very low thickness and the high surface roughness of ITO. Fortunately, in a previous report, the work function of an ultra-thin Al_2O_3 layer was determined using SKPM, which thus proved to be an efficient technique of ultra-thin Al_2O_3 layer characterization.

Figure 4(b) shows the surface morphology and SKPM images of the boundary between Al_2O_3-

coated ITO (upper region) and the ITO substrate (lower region). The latter images express the difference of surface potential, and the contrast between the area covered by Al_2O_3 and the ITO substrate thus confirms that Al_2O_3 was well deposited. Differences between the work functions of pristine ITO– and Al_2O_3-covered areas for various *n* were calculated from SKPM data and are shown in **Figure S2**. The above difference decreased with increasing *n*, in agreement with the results of previous studies (11, 29).

In addition, we used atomic force microscopy (AFM) to characterize the etching of PEDOT:PSS-exposed bare and Al_2O_3-coated ITO surfaces placed on a 130 °C hot plate (i.e., under conditions identical to those used for device fabrication). **Figure S3** shows the obtained surface morphology differences and surface roughness values before and after exposure to PEDOT:PSS, revealing that the root-mean-square (RMS) surface roughness of ITO increased from 1.56 to 3.72 nm after etching by PEDOT:PSS, whereas almost no surface roughness change was observed for Al_2O_3-covered surfaces (e.g., 1.66 and 1.74 nm, respectively, for n = 4). This behavior suggested that the Al_2O_3 layer effectively suppressed the etching reaction with PEDOT:PSS.

As stated above, the best QLED performance was obtained for n = 4, which was ascribed to the mechanism of Al_2O_3 growth. During ALD, the first layer of Al_2O_3 forms Al–O bonds via OH groups and defect sites on the surface. Although the ALD technology is known to achieve high coating coverage, it is difficult to form a perfect two-dimensional (2D) layer with 100% coverage in one cycle because of the complex growth conditions (19, 30). Therefore, during the initial few cycles, Al_2O_3 layers were formed based on the island growth mechanism as a prelude to 2D layer formation. Thus, the time when the thinnest Al_2O_3 2D layer begins to form was concluded to correspond to n = 4.

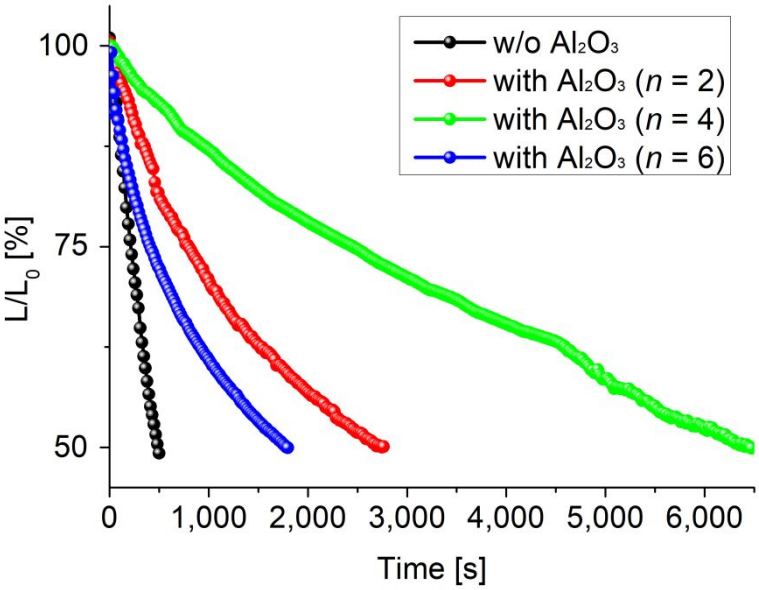

Figure 5. Performance degradation of QLEDs prepared using different *n*.

Figure 5 shows the results of lifetime measurements. In general, QLED lifetime is defined as the

time required for the initial luminance of L_0 (1,000 cd/m^2 in our case) to decrease by a factor of two during continuous operation at a constant bias. In these measurements, all devices without any encapsulation were characterized under the same environmental conditions (temperature, humidity, etc.) in an atmospheric dark box. Notably, all Al_2O_3-containing QLEDs featured longer lifetimes than the QLED without Al_2O_3. Particularly, the n = 4 device had the longest lifetime of 6,472 s, which was ~13 times larger than that of the Al_2O_3-free QLED. At this point, it is worth mentioning that no encapsulation process was applied in this study. Actually, we previously tried to enhance the lifetime of our devices by simple glass encapsulation, but found that this method is inadequate, since ZnO NPs used in our devices as the ETL might get damaged by UV light during sealant UV-curing. However, we anticipate that device lifetime can be further increased if an encapsulation method suitable for our device structure is developed.

The enhancement of QLED luminance, current efficiency, and lifetime by application of an Al_2O_3 layer as a metal ion diffusion barrier is an interesting result that can possibly aid the commercialization of QLEDs. In particular, the developed coating procedure can be performed at a low temperature of ~150 °C and can therefore be applied not only to rigid ITO glass substrates but also to flexible substrates such as polyethylene terephthalate (PET) and polyethylene naphthalate (PEN). The typical characteristics of flexible QLEDs are shown in **Figure S4**, while **Figures S5(a)** and **(b)** show the emission images of glass- and PEN-based QLEDs, respectively, supporting the hypothesis that the Al_2O_3 layer deposition technique can be applied to flexible substrates.

Conclusions

In this study, QLED characteristics were improved via ALD-based insertion of Al_2O_3 as a metal diffusion barrier at the interface between PEDOT:PSS and the ITO anode of conventional-structure green QLED. To determine whether the ultra-thin Al_2O_3 layer was well deposited on the ITO surface, we confirmed the surface potential difference between bare and Al_2O_3-coated ITO by SKPM and have further optimized the thickness of Al_2O_3, aiming to achieve a value that was as small as possible but allowed for uniform ITO surface coverage. As a result, the best characteristics (maximum luminance = 39,410 cd/m^2, maximum current efficiency = 47.89%, maximum EQE = 12.89%) were observed for the QLED prepared using four Al_2O_3 deposition cycles. The enhanced performance was primarily ascribed to the prevention of ITO etching by PEDOT:PSS and the decreased extent of metal ion diffusion into the EML. The results of the PEDOT:PSS etching test showed that the above etching increased the RMS roughness and changed the surface morphology of bare ITO, while these effects were negligible in the case of Al_2O_3-coated ITO. In addition, the effective blockage of metal ion migration during device operation by Al_2O_3 was confirmed by (a) TR-PL measurements, which revealed that exciton

quenching was suppressed in the device with Al_2O_3, and (b) the results of EDS analysis, which showed that no signals of metal species were observed in the EML layer of Al_2O_3-coated QLEDs. Thus, the adopted approach can aid QLED commercialization and is expected to be applicable to next-generation flexible devices that can be used at low temperatures.

Supporting Information Available: Additional characterization of as-fabricated QLEDs. This material is available free of charge via the Internet at http://pubs.acs.org.

Notes

The authors declare no competing financial interest.

Acknowledgments

This research was supported by the Pioneer Research Center Program through the National Research Foundation of Korea Funded by the Ministry of Science and ICT (NRF-2014M3C1A3053029).

References

1. Jiang, C.; Zhong, Z.; Liu, B.; He, Z.; Zou, J.; Wang, L.; Wang, J.; Peng, J.; Cao, Y. Coffee-Ring-Free Quantum Dot Thin Film Using Inkjet Printing from a Mixed-Solvent System on Modified ZnO Transport Layer for Light-Emitting Devices. *ACS Appl. Mater. Interfaces* **2016,** *8*, 26162-26168.

2. Kim, J.; Lee, J.; Son, D.; Choi, M. K.; Kim, D.-H. Deformable Devices with Integrated Functional Nanomaterials for Wearable Electronics. *Nano Convergence* **2016,** *3*, 4.

3. Lee, K.-H.; Lee, J.-H.; Song, W.-S.; Ko, H.; Lee, C.; Lee, J.-H.; Yang, H. Highly Efficient, Color-Pure, Color-Stable Blue Quantum Dot Light-Emitting Devices. *ACS Nano* **2013,** *7*, 7295-7302.

4. Mashford, B. S.; Stevenson, M.; Popovic, Z.; Hamilton, C.; Zhou, Z.; Breen, C.; Steckel, J.; Bulovic, V.; Bawendi, M.; Coe-Sullivan, S.; Kazlas, P. T. High-Efficiency Quantum-Dot Light-Emitting Devices with Enhanced Charge Injection. *Nat. Photonics* **2013,** *7*, 407-412.

5. Tang, C. W.; Vanslyke, S. A. Organic Electroluminescent Diodes. *Appl. Phys. Lett.* **1987,** *51*, 913-915.

6. Liu, S.; Liu, W.; Ji, W.; Yu, J.; Zhang, W.; Zhang, L.; Xie, W. Top-Emitting Quantum Dots Light-Emitting Devices Employing Microcontact Printing with Electricfield-Independent Emission. *Sci. Rep.* **2016,** *6*, 22530.

7. Shirasaki, Y.; Supran, G. J.; Bawendi, M. G.; Bulovic, V. Emergence of Colloidal Quantum-

Dot Light-Emitting Technologies. *Nat. Photonics* **2013,** *7*, 13-23.

8. Scholz, S.; Kondakov, D.; Lüssem, B.; Leo, K. Degradation Mechanisms and Reactions in Organic Light-Emitting Devices. *Chem. Rev.* **2015,** *115*, 8449-8503.

9. Park, Y. R.; Doh, J. H.; Shin, K.; Seo, Y. S.; Kim, Y. S.; Kim, S. Y.; Choi, W. K.; Hong, Y. J. Solution-Processed Quantum Dot Light-Emitting Diodes with PANI:PSS Hole-Transport Interlayers. *Org. Electron.* **2015,** *19*, 131-139.

10. Dai, X. L.; Zhang, Z. X.; Jin, Y. Z.; Niu, Y.; Cao, H. J.; Liang, X. Y.; Chen, L. W.; Wang, J. P.; Peng, X. G. Solution-Processed, High-Performance Light-Emitting Diodes Based on Quantum Dots. *Nature* **2014,** *515*, 96-99.

11. Zhou, L.; Zhuang, J. Y.; Tongay, S.; Su, W. M.; Cui, Z. Performance Improvement of Organic Light Emitting Diode with Aluminum Oxide Buffer Layer for Anode Modification. *J. Appl. Phys.* **2013,** *114*, 074506.

12. Bae, W. K.; Park, Y.-S.; Lim, J.; Lee, D.; Padilha, L. A.; McDaniel, H.; Robel, I.; Lee, C.; Pietryga, J. M.; Klimov, V. I. Controlling the Influence of Auger Recombination on the Performance of Quantum-Dot Light-Emitting Diodes. *Nat. Commun.* **2013,** *4*, 2661.

13. Li, Z. Enhanced Performance of Quantum Dots Light-Emitting Diodes: The Case of Al_2O_3 Electron Blocking Layer. *Vacuum* **2017,** *137*, 38-41.

14. Kim, D.; Fu, Y.; Kim, J.; Lee, K.; Kim, H.; Yang, H.; Chae, H. Improved Electroluminescence of Quantum Dot Light-Emitting Diodes Enabled by a Partial Ligand Exchange with Benzenethiol. *Nanotechnology* **2016,** *27*, 245203.

15. Lim, J.; Park, M.; Bae, W. K.; Lee, D.; Lee, S.; Lee, C.; Char, K. Highly Efficient Cadmium-Free Quantum Dot Light-Emitting Diodes Enabled by the Direct Formation of Excitons within InP@ZnSeS Quantum Dots. *ACS Nano* **2013,** *7*, 9019-9026.

16. Sharma, A.; Andersson, G.; Lewis, D. A. Role of Humidity on Indium and Tin Migration in Organic Photovoltaic Devices. *Phys. Chem. Chem. Phys.* **2011,** *13*, 4381-4387.

17. Chambers, B. A.; Macdonald, B. I.; Ionescu, M.; Deslandes, A.; Quinton, J. S.; Jasieniak, J. J.; Andersson, G. G. Examining the Role of Ultra-Thin Atomic Layer Deposited Metal Oxide Barrier Layers on CdTe/ITO Interface Stability during the Fabrication of Solution Processed Nanocrystalline Solar Cells. *Sol. Energy Mater. Sol. Cells* **2014,** *125*, 164-169.

18. Groner, M. D.; Fabreguette, F. H.; Elam, J. W.; George, S. M. Low-Temperature Al_2O_3 Atomic Layer Deposition. *Chem. Mater.* **2004,** *16*, 639-645.

19. Puurunen, R. L. Surface Chemistry of Atomic Layer Deposition: A Case Study for the Trimethylaluminum/Water Process. *J. Appl. Phys.* **2005,** *97*, 121301.

20. Lin, Y.-Y.; Chang, Y.-N.; Tseng, M.-H.; Wang, C.-C.; Tsai, F.-Y. Air-Stable Flexible Organic Light-Emitting Diodes Enabled by Atomic Layer Deposition. *Nanotechnology* **2015,** *26*, 024005.

21. Ji, W.; Liu, S.; Zhang, H.; Wang, R.; Xie, W.; Zhang, H. Ultrasonic Spray Processed, Highly Efficient All-Inorganic Quantum-Dot Light-Emitting Diodes. *ACS Photonics* **2017,** *4*, 1271-1278.

22. French, R. H. Electronic Band Structure of Al_2O_3, with Comparison to Alon and AIN. *J. Am. Ceram. Soc.* **1990,** *73*, 477-489.

23. Ealet, B.; Elyakhloufi, M. H.; Gillet, E.; Ricci, M. Electronic and Crystallographic Structure of Gamma-Alumina Thin Films. *Thin Solid Films* **1994,** *250*, 92-100.

24. Toyoda, S.; Shinohara, T.; Kumigashira, H.; Oshima, M.; Kato, Y. Significant Increase in Conduction Band Discontinuity Due to Solid Phase Epitaxy of Al_2O_3 Gate Insulator Films on GaN Semiconductor. *Appl. Phys. Lett.* **2012,** *101*, 231607.

25. Afanas'ev, V. V.; Houssa, M.; Stesmans, A.; Heyns, M. M. Band Alignments in Metal-Oxide-Silicon Structures with Atomic-Layer Deposited Al_2O_3 and ZrO_2. *J. Appl. Phys.* **2002,** *91*, 3079-3084.

26. Filatova, E. O.; Konashuk, A. S. Interpretation of the Changing the Band Gap of Al_2O_3 Depending on Its Crystalline Form: Connection with Different Local Symmetries. *J. Phys. Chem. C* **2015,** *119*, 20755-20761.

27. Rose, V.; Franchy, R. The Band Gap of Ultrathin Amorphous and Well-Ordered Al_2O_3 Films on CoAl(100) Measured by Scanning Tunneling Spectroscopy. *J. Appl. Phys.* **2009,** *105*, 7-10.

28. Pacholski, C.; Kornowski, A.; Weller, H. Self-Assembly of ZnO: From Nanodots to Nanorods. *Angew. Chem., Int. Ed.* **2002,** *41*, 1188-1191.

29. Zhou, Y.; Cheun, H.; Potscavage Jr, W. J.; Fuentes-Hernandez, C.; Kim, S.-J.; Kippelen, B. Inverted Organic Solar Cells with ITO Electrodes Modified with an Ultrathin Al_2O_3 Buffer Layer Deposited by Atomic Layer Deposition. *J. Mater. Chem.* **2010,** *20*, 6189-6194.

30. Naumann, V.; Otto, M.; Wehrspohn, R. B.; Werner, M.; Hagendorf, C. Interface and Material Characterization of Thin ALD-Al_2O_3 layers on Crystalline Silicon. *Energy Procedia* **2012,** *27*, 312-318.

For Table of Contents Use Only

Title: Insertion of an inorganic barrier layer as a method of improving the performance of quantum dot light-emitting diodes

Authors: Sang Hyun Yoon, Dham Gwak, Hong Hee Kim, Hwi Je Woo, Jinhee Cho, Jin Woo Choi, Won Kook Choi, Young Jae Song, Chang-Lyoul Lee, Jongnam Park, Kwang Heo, and Young Jin Choi

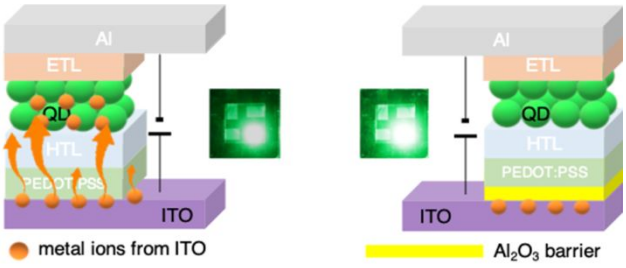

Enhanced performance of conventionally structured QLED by Insertion of Al_2O_3 layer as metal ion diffusion barrier between ITO and PEDOT:PSS